KCI CONRETE JOURNAL
Vol.14 No.4, Dec., 2002, pp.139-144

Experiment of Compressive Strength Enhancement of Circular Concrete Column Confined by Carbon Tubes

Won-Kee Hong[1)*], Hee-Cheul Kim[1)], and Suk-Han Yoon[1)]

[1)] *Department of Architectural Engineering, Kyunghee University, Korea*

(Received June 10, 2002; Accepted December 20, 2002)

Abstract

Concrete filled FRP tube has lately attracted attention as the member that can substitute the conventional reinforced concrete. Glass fiber and carbon fiber are some of available materials for FRP tube. Carbon tube is filament wound with specified winding angle to meet the appropriate capacity demands. Confinement effect of carbon tube is varied according to winding angle. In this study, a total 4 of large scale circular specimens of 30cm diameter and 60cm height is tested. To estimate the effect of winding angle and thickness of carbon tube on the increased confined compressive strength, the test tube are wound with ±45°and ±30°with two types of thickness, 2mm and 3mm, respectively. It is shown that effectively increased confined strength and ductility are observed from the specimens with ±45° winding angle than ±30°winding angle. Increasing thickness is not as effective as adjusting winding angle for the confinement of concrete core.

Keywords: carbon tube, confinement, winding angle, compressive strength, ductility

1. Introduction

Composite structure such as concrete filled steel tube is recognized for effective structural system. Especially in seismic regions it is very effective due to its high strength and ductility. The steel tube enhances not only strength and ductility of columns by confining concrete core also shear and flexural strength. Concrete core prevents steel tube from buckling. But since the steel is isotropic material, its resistance in the axial and circumferential direction cannot be optimized. Most of axial forces are resisted by steel due to its high modulus resulting in premature buckling may occurred in steel tube. In early loading stage, since the Poisson's ratio of steel is larger than that of concrete, partial separation of the two materials may occur and consequently the activation of confinement mechanism is delayed. Finally, its heavy-weight causes additional load and out door use of steel tubes in corrosive environments need additional expenses.

FRP(Fiber Reinforced Polymer) may be used to solve these problems. Effective composite structure can be achieved by combining the mass, stiffness, damping and low cost of concrete with the speed of construction, lightweight, strength and durability of FRP. Since FRP is anisotropic material, its resistance in any directions are optimized for required capacity. Most of studies for composite structure deal with glass-fibers while the studies dealing with carbon fibers are not carried as many as those for glass fiber. Moreover, most of the studies for both glass fiber and carbon fiber are not for the new construction but for retrofitting and strengthening.

The existing studies used FRP tubes which are manufactured by filament wound with constant winding angle to evaluate the confinement effect. Specimens used in the existing studies are such a small scale that they cannot account for the size effect for large scale specimens resulting in overestimating the capacity of actual columns.

In this study, the winding angle of fiber is combined for each orientation with thickness. The size of specimen is large scale that can reflect the behavior of actual column more precisely.

* *Corresponding author*
Tel.: +82- 31-201-2069; Fax.: +82-31- 202-2107
E-mail address: Hongwk@khu.ac.kr

2. Experimental work

2.1 Carbon tubes

Carbon fiber for tubes is HTA-12K imported from Toho Tenex, Co. Japan. Matrix is composed of SS-2018W (polyester epoxy resin), SS-2010H(hardener), and SA-101 (accelerator) made by SNS Chemical, Korea. Material properties for fiber and resin are shown in Table 1.

Tubes are filament-wound carbon composite using mandrel with winding angle that is pre-decided. Fig. 1 and 2 show the filament winding process and the circular carbon tubes.

2.2 Specimens

Four large-scale of 600mm height by 300mm diameter circular columns confined by carbon composite tubes are tested. The specification of specimens are shown in Table 2. Carbon tubes have some errors in actual thickness about 0.5mm. Target strength of concrete is 26.5MPa. The average strength of concrete cylinders is about 25.8Mpa.

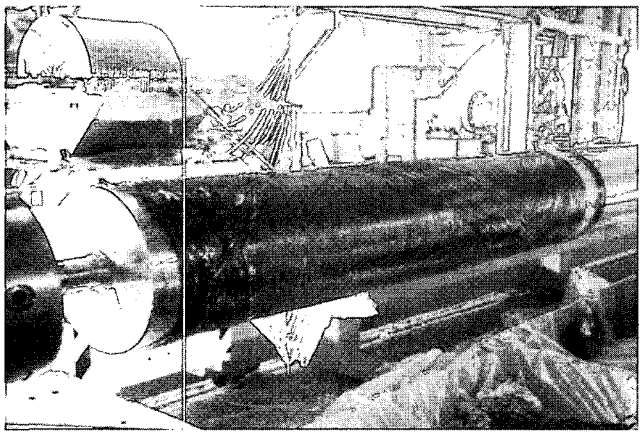

Fig. 1 Filament winding process

Fig. 2 Carbon tubes

2.3 Instrumentation

For the measurement of lateral and axial strain, each specimen is instrumented by a total of twelve 10mm bi-axial surface gage. Three gages are attached at 50mm from the top face, mid-height, and 50mm from the bottom face with 90° apart in circumferential direction. The additional 70mm strain gage is embedded in concrete core to obtain accurate axial strain. Four linear variable displacement transducers(LVDT) are also installed at 90° apart around specimen to measure average axial displacement and strain which is compared with the data obtained from strain gages. A 10000kN capacity of UTM for loading and UCAM-500A data acquisition system for obtaining data are used. Fig. 3 shows instrumentation of Specimen C45-3T. The uni-axial load is applied under displacement control with constant rate of 0.01mm/sec.

Table 1 Material properties

	Carbon fiber	Resin
Gravity	1.76	1.2
Tensile strength(MPa)	3920	64~74
Tensile modulus(GPa)	235	
Elongation(Ultimate strain)	0.017	0.02~0.03

Table 2 Specimen program

Specimen designation	f'_c (MPa)	Thickness by winding angle			Total
		90°	45°	30°	
C30-2T	26.5	1		1	2
C30-3T	26.5	1		2	3
C45-2T	26.5	1	1		2
C45-3T	26.5	1	2		3

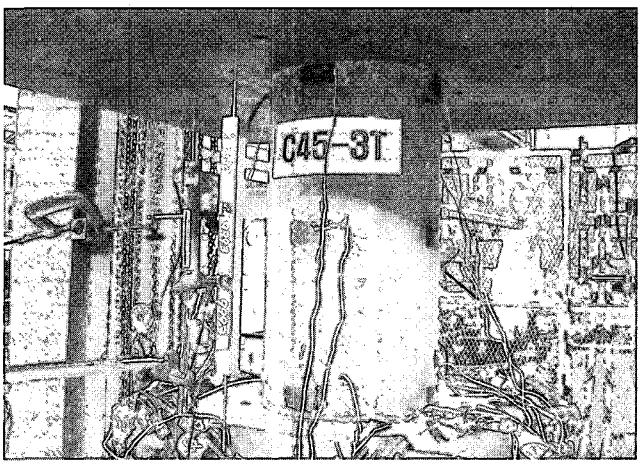

Fig. 3 Instrumentation of specimen C45-3T

3. Experimental results

3.1 Stress-strain relationships

Table 3 presents a summary of test results. Compressive strength of concrete, f_{co}, is defined when axial strain is 0.002. Carbon tube intercepts ventilation so that the compressive strength of concrete is lower than that of cylinder tests. f_{cc} is compressive strength of confined concrete and ε_{cc} is ultimate strain of confined concrete.

The failure occurs near the mid-height of specimen. Cracking sound was heard due to micro cracks of concrete and shifting of aggregates until middle stage of loading. After then snapping sounds occurs due to partial fracture of carbon fiber intermittently. Finally, specimens are fractured with explosive sound.

Fig. 4 shows stress-strain curves for each specimens. The left side of axis is the lateral stress-strain relationships and the right side is the axial one. In Fig. 5 axial stresses and strains are normalized with respect to the stress at the strain of 0.002. The maximum increase of strength and strain are 2.86 and 22.5 times those of unconfined concrete in Specimen C45-3T.

As shown in Fig. 4 and Fig. 5, the strength and the ductility of confined concrete are increased as the orientation of carbon fabric toward circumferential direction of columns. The specimens, C30 series, do not demonstrate the increase of ductility as the thickness of tube increases but the ductility of the specimens, C45 series, increased significantly as the thickness increased. This is because the fiber oriented circumferential direction (90°) is not increased but the fiber oriented 30° and 45° is increased. The fiber oriented 45° can resist the stress of circumferential component more effectively than the fiber oriented with 30°. The stress-strain curves show three distinct regions. The initial linear region depends on the behavior of unconfined concrete followed by transition zone. In the final zone where confinement provided by tubes, stress-strain curves are increased monotonically until the failure of specimens. In this region the behavior of CFCT is dominated by carbon tube.

Table 3 Summary of test results

	f_{co} (MPa)	f_{cc} (MPa)	ε_{cc}	f_{cc}/f_{co}	$\varepsilon_{cc}/0.002$
C30-2T	23.3	45.7	0.029	1.96	14.5
C30-3T	21.3	46.6	0.028	2.18	14.0
C45-2T	23.1	60.1	0.039	2.60	19.5
C45-3T	20.7	59.1	0.045	2.86	22.5

3.2 Failure mechanism

The failure modes of specimens are different for C45 and C30. As shown in Fig. 6 and Fig. 7, the specimens of C30 series are fractured with wide ring breakage, and the specimens of C45 series are with narrow ring breakage. The

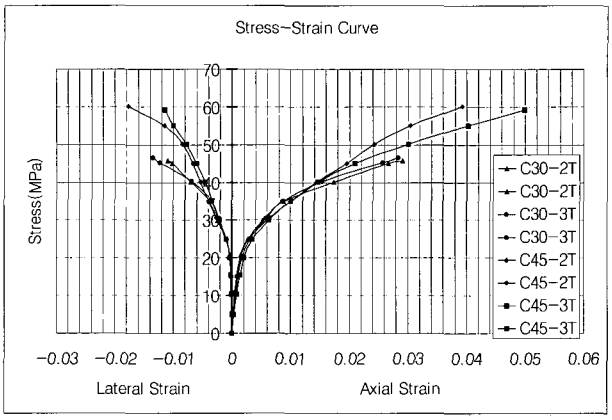

Fig. 4 Experimental stress-strain curves

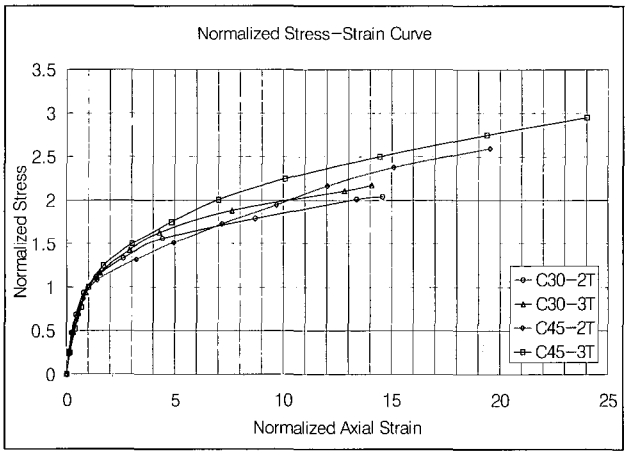

Fig. 5 Normalized stress-strain curves

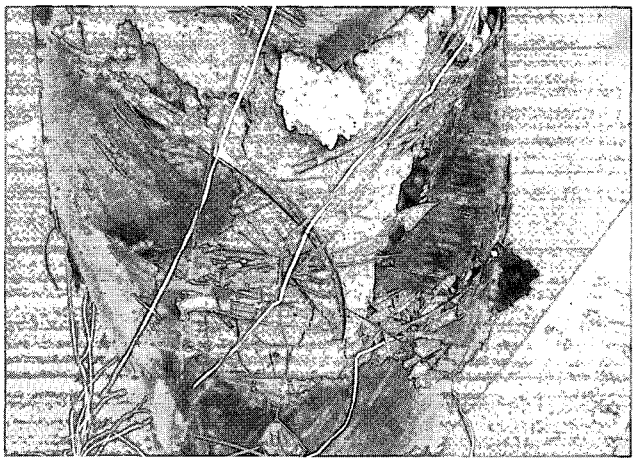

Fig. 6 Failure of C30-3T

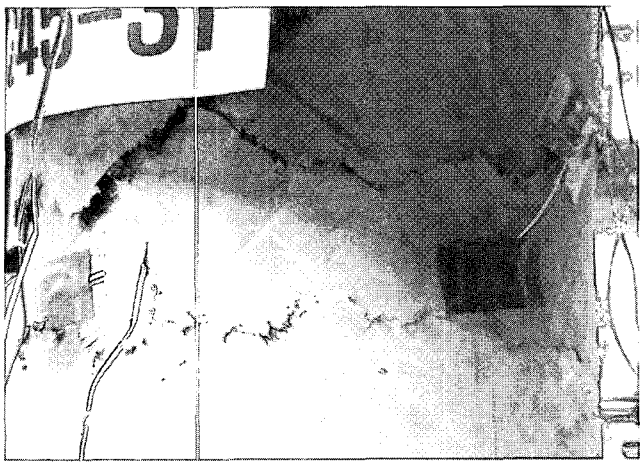

Fig. 7 Failure of C45-3T

specimens of C30 failed suddenly and catastrophically than those of C45. Concrete core in the specimen of C30 was separated into two pieces in cone shape resulting from violently fracture of carbon tube (Fig. 8). The specimens of C45 are cracked in a circumferential direction due to relatively less severe fracture of carbon tube (Fig. 9).

Fig. 10 shows microscopic examination of carbon composite fibers by scanning electron microscope(SEM). The broken piece of carbon composite tubes magnified by one thousand times is compared with the undamaged part of carbon tubes. Carbon filaments of undamaged tube specimen are not visible since carbon filaments are impregnated and covered by epoxy resin.

However, filament of Fig. 10(a) can be seen clearly because the resin was spalled due to the tensile stress developed during adjacent carbon rupture. Fig. 10(a) is carbon composite fiber taken from Specimen C30-2T, showing a filament of about $7\mu m$ diameter. The damaged fibers of Specimen C30-3T are shown in Fig. 10(b) where the extensive fiber debonding and delamination occur at the inner carbon layers of 90° fiber orientation. In this photo, split of about $7\mu m$ width is found along fibers of 30° winding orientation, indicating that the fibers of outer layer with 30° winding orientation do not resist lateral pressure effectively during the rupture of fibers.

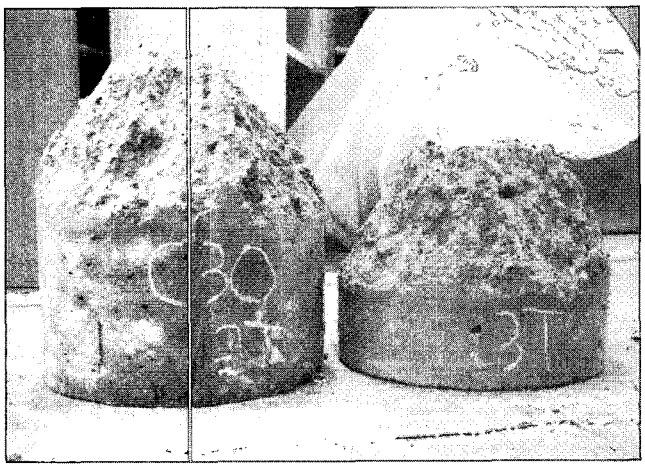

Fig. 8 Failure of concrete core in C30-3T

Fig. 9 Failure of concrete core in C45-3T

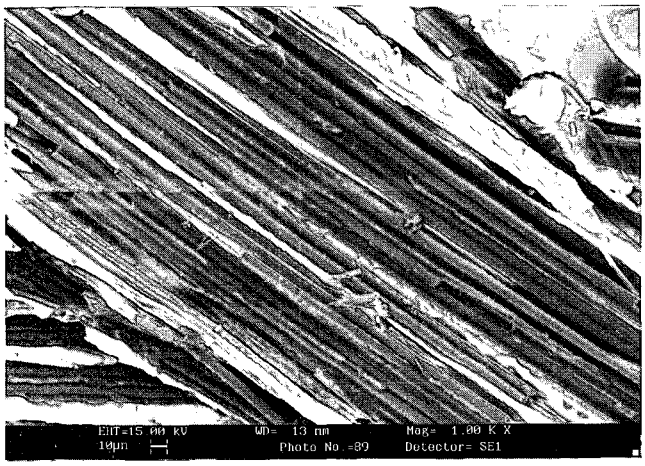

Fig. 10 (a) Undamaged carbon tube of C30-2T

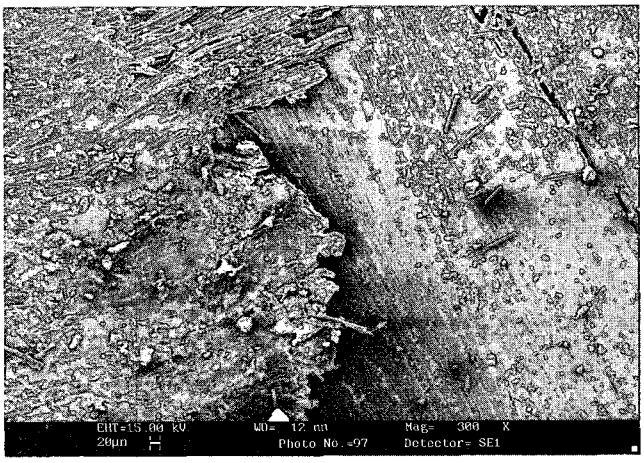

Fig. 10 (b) Damaged carbon tube of C30-3T

3.3 Existing confinement model

Fardis et al.(1981)[1] developed equations to model con crete specimen encased in fiber glass-reinforced plastic subjected to uniaxial compression loads. They concluded that FRP-encased concrete could provide economic solution with significantly improved strength and ductility. FRP-encased concrete with three types of fibers was tested by Nanni and Bradford(1995).[2] Three types of fibers were aramid FRP, filament-wound E-glass, and hybrid glass-aramid FRP shells. Recently, Samann et al(1998)[3] proposed equations to predict the complete bilinear stress-strain curve of FRP-confined concrete in both axial and lateral directions. Table 4 shows the summary of existing confining models. Experimental results are compared with existing confining model (Fig. 11 and Fig. 12). As shown in these figures, confining model by Karbhari et al(1993)[4] overestimates the strength but underestimates the ductility. The rest of the confining models overestimate the both strength and ductility for Specimen C30-3T. Existing confining models did not adequately predict the behavior of concrete column confined by carbon tube.

Table 4 Existing confining models for concrete

Proposer	Equations
Mander (1988) [5]	$f_{cc} = f_{co}(-1.254 + 2.254\sqrt{1 + 7.94 f_l / f_{co}} - 2 f_l / f_{co})$
	$\varepsilon_{cc} = \varepsilon_{co}(1 + 5(f'_{cc} / f'_{co}))$
Fardis (1981) [1]	$f'_{cc} = f'_{co}(1 + 4.1(\frac{t_{cf} f_j}{D f'_{co}}))$
	$\varepsilon_{cc} = \varepsilon_{co} + 0.001(\frac{E_j t_{cf}}{D f'_{co}})$
Karbhari (1993) [4]	$f_{cc} = f_{co}(1 + 2.1(\frac{2 t_{cf} f_j}{D f'_{co}})^{0.87})$
	$\varepsilon_{cc} = \varepsilon_{co} + 0.01\frac{2 t_{cf} f_j}{D f'_{co}}$
Samaan (1998) [3]	$f_{cc} = f_{co} + 0.6 f_l^{0.7}[MPa] = f_{co} + 3.38 f_l^{0.7}[ksi]$
	$\varepsilon_{cc} = \frac{f_{co} - f_0}{E_2}$ $\quad f_0 = 0.872 f'_{co} + 0.371 fi + 6.258[MPa]$
	$E_2 = 245.61 f'^{0.2}_{co} + 1.3456\frac{E_j t_{cf}}{D}[MPa]$

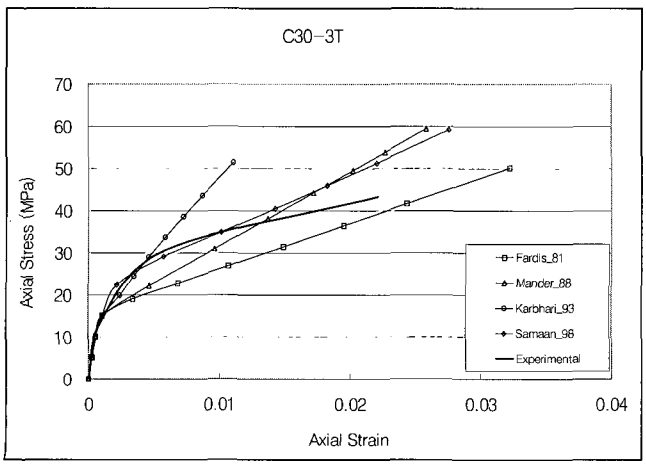

Fig. 11 Comparisons with confining model (C30-3T)

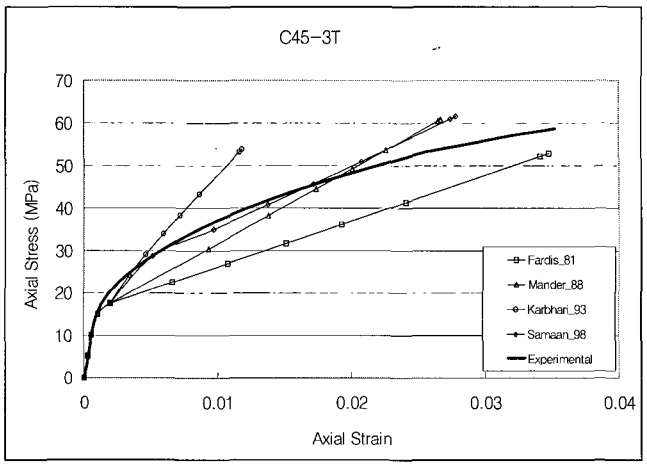

Fig. 12 Comparison of confining model (C45-3T)

4. Conclusions

In the present study large scale circular columns confined by carbon composite tube were tested with monotonically increasing axial load to eliminate the effect which can be caused by testing small scale specimen. Significant enhancement of strength and ductility is achieved by confining concrete core with carbon composite tube.

The carbon tubes with 45° winding orientation confined concrete core more effectively than the carbon tubes with 30° angle. Strength and ductility of specimens varied by orientation of fiber rather than thickness of tube. Because 1mm thickness was too thin to study the confinement effect. The existing confining models for concrete could not predict, behavior of a column confined by carbon composite tube properly.

Acknowledgements

The authors would like to thank Kyung-Hee University, Korea, for the financial supports.

References

1. Fardis, M. N. and Khalili, H., "Concrete encased in fiberglass-reinforced plastic," *ACI Structural Journal*, November-December, 1981.
2. Nanni A, Bradford NM. FRP jacketed concrete under uniaxial compression, *Construction and Building Materials*, 1995, Vol. 9, No. 2, pp. 115-124.
3. Samaan, M., Mirmiran, A., and Shahawy, M., "Model of concrete confined by composites," *Journal of Structural Engineering*, ASCE, Vol 124, No. 9, September, 1998.
4. Karbhari, V. M. and Eckel, D., "Strengthening of concrete column stubs through resin-infused composite wraps," *Journal of Thermoplastic Composite Materials*, No. 6, April, 1993.
5. Mander, J. B., Priestley, M. J. N., and Park, R. J. T., "Theoretical stress-strain model for confined concrete." *Journal of Structural Engineering*, ASCE, Vol. 114, No. 8, August, 1998.
6. Park, R. and Paulay, T. "*Reinforced concrete structures*," John Wiley & Sons. 1975.